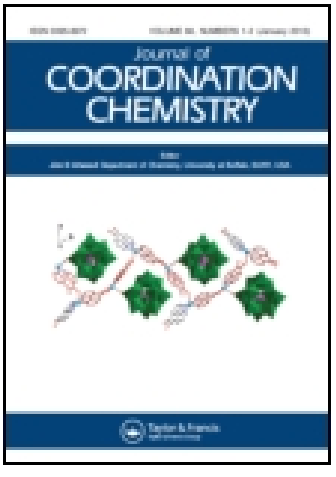

Journal of Coordination Chemistry
Publication details, including instructions for authors and subscription information:
http://www.tandfonline.com/loi/gcoo20

A complex of ceftriaxone with Pb(II): synthesis, characterization, and antibacterial activity study

Aleksandr O. Lykhin[ab], Galina V. Novikova[a], Alexander A. Kuzubov[acd], Natalia A. Staloverova[a], Natalia I. Sarmatova[a], Sergey A. Varganov[e] & Pavel O. Krasnov[d]

[a] Department of Chemistry, Siberian Federal University, Krasnoyarsk, Russia

[b] Information Sciences and Telecommunication Institute, Siberian State Aerospace University, Krasnoyarsk, Russia

[c] L.V. Kirensky Institute of Physics, Siberian Branch of the Russian Academy of Sciences, Krasnoyarsk, Russia

[d] Department of Physics, Siberian State Technological University, Krasnoyarsk, Russia

[e] Department of Chemistry, University of Nevada, Reno, Reno, NV, USA

Accepted author version posted online: 23 Jun 2014.Published online: 16 Jul 2014.

To cite this article: Aleksandr O. Lykhin, Galina V. Novikova, Alexander A. Kuzubov, Natalia A. Staloverova, Natalia I. Sarmatova, Sergey A. Varganov & Pavel O. Krasnov (2014) A complex of ceftriaxone with Pb(II): synthesis, characterization, and antibacterial activity study, Journal of Coordination Chemistry, 67:16, 2783-2794, DOI: 10.1080/00958972.2014.938065

To link to this article: http://dx.doi.org/10.1080/00958972.2014.938065

Journal of Coordination Chemistry, 2014
Vol. 67, No. 16, 2783–2794, http://dx.doi.org/10.1080/00958972.2014.938065

A complex of ceftriaxone with Pb(II): synthesis, characterization, and antibacterial activity study

ALEKSANDR O. LYKHIN*†‡, GALINA V. NOVIKOVA†, ALEXANDER A. KUZUBOV†§¶, NATALIA A. STALOVEROVA†, NATALIA I. SARMATOVA†, SERGEY A. VARGANOV‖ and PAVEL O. KRASNOV¶

†Department of Chemistry, Siberian Federal University, Krasnoyarsk, Russia
‡Information Sciences and Telecommunication Institute, Siberian State Aerospace University, Krasnoyarsk, Russia
§L.V. Kirensky Institute of Physics, Siberian Branch of the Russian Academy of Sciences, Krasnoyarsk, Russia
¶Department of Physics, Siberian State Technological University, Krasnoyarsk, Russia
‖Department of Chemistry, University of Nevada, Reno, Reno, NV, USA

(*Received 30 January 2014; accepted 18 May 2014*)

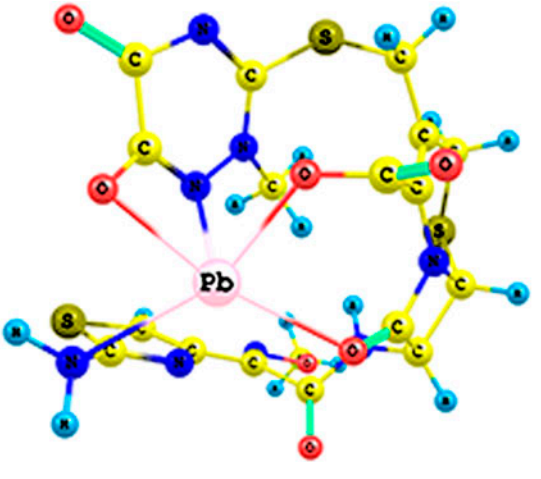

A Pb(II) complex with ceftriaxone (H_2Ceftria) antibiotic was synthesized by reaction of ceftriaxone disodium salt (hemi)heptahydrate with lead nitrate in water–ethanol medium. The complex was characterized on the basis of complexometric titration, spectrophotometric and thermogravimetric analyses, capillary electrophoresis, IR, Raman and UV–vis spectroscopies, and density functional theory calculations. Pb(II) is five-coordinate with distorted square pyramidal geometry. The coordination of $Ceftria^{2-}$ to Pb(II) occurs through N and O of the triazine, lactam carbonyl, carboxylate, and amine groups. The antibacterial activity study showed that *Klebsiella pneumoniae* is resistant to [Pb(Ceftria)]·3H_2O. The antibacterial activity of [Pb(Ceftria)]·3H_2O against *Staphylococcus aureus* is

*Corresponding author. Email: alykhin@sfu-kras.ru

reduced compared with ceftriaxone. In contrast, the antibacterial activity of [Pb(Ceftria)]·3H_2O against *Escherichia coli* is 28% higher than that of ceftriaxone antibiotic.

Keywords: Ceftriaxone lead(II) complex; DFT; IR spectroscopy; TGA; Antibacterial screening

1. Introduction

Cephalosporins are semisynthetic broad-spectrum antibiotics chemically related to penicillins, that predetermines a similar mechanism of their antimicrobial activity, mechanism of resistance, and other properties [1–4]. Ceftriaxone antibiotic (figure 1) belongs to the third generation of cephalosporins. The bactericidal activity of ceftriaxone is caused by its inhibition of the synthesis of the bacterial cell wall [5]. Ceftriaxone forms a stable acyl-enzyme intermediate, which suppresses peptidoglycan cross-linking, thereby disrupting the cell wall structural integrity [6–8].

Ceftriaxone is stable with respect to β-lactamases, produced by most Gram-positive and Gram-negative bacteria, and is used in the therapy of neonates [9]. However, the evolution of the bacterial resistance mechanisms necessitates the search for more effective antibiotics to overcome action of β-lactamases [10], especially extended spectrum β-lactamase [11, 12] and metallo-β-lactamases containing Zn(II), Co(II) and Cd(II) ions [13–15]. In the presence of these enzymes, cephalosporins, like other β-lactams, undergo the β-lactam ring opening [16]. Another important mechanism of bacterial resistance which must be overcome is the production of alternative penicillin-binding proteins 2 with lower affinity to antibiotics [17, 18].

There are several ways to increase antibacterial activity of the β-lactams. For example, combining β-lactams with β-lactamase inhibitors sometimes can be an effective strategy. This approach, however, is not universal because of a wide variety of β-lactamase species [19, 20]. Another promising strategy is to target the bacterial regulatory systems responsible for β-lactamase expression [2]. Arguably, the simplest approach to enhancing the antibacterial properties of existing antibiotics is creating their complexes with different metal ions [21–23].

Metal complexes of ceftriaxone have both toxicological and pharmacological properties [24]. While the interaction between ceftriaxone and metal ions can lead to precipitation that results in serious adverse drug events [25], complexes of cephalosporins with Cu(II) are

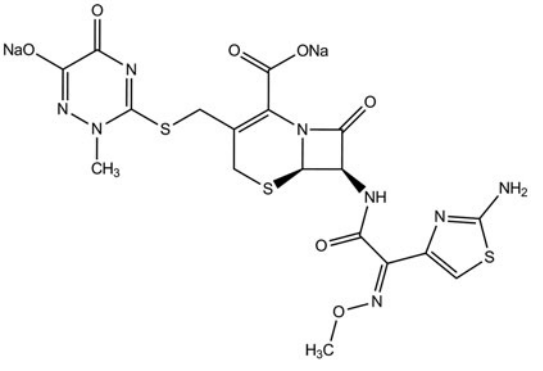

Figure 1. Structure of ceftriaxone disodium salt.

widely studied and used in treatment of diseases such as rheumatoid arthritis [26, 27]. In general, the antibacterial properties of ceftriaxone complexes can increase or decrease relative to pure ceftriaxone [24]. The synthesis of such metal–antibiotic complexes is an important area of medicinal chemistry [27–32].

Here, we report the synthesis and characterization of a Pb(II) complex with ceftriaxone (H_2Ceftria) antibiotic. The structure of the new complex was studied using a combination of experimental and computational techniques. In addition, the antibacterial activity of the complex against several Gram-positive and Gram-negative bacteria was investigated.

2. Experimental

2.1. *Materials and methods*

All chemicals were obtained in pure form and used without purification. [Pb(Ceftria)]·3H_2O was obtained by mixing the ceftriaxone disodium salt (hemi)heptahydrate (0.3 g; 4.52×10^{-4} M) with lead nitrate (0.15 g; 4.52×10^{-4} M) in water-ethanol medium (1 : 1). The reaction mixture was left in a dark place at room temperature for 30 min. The formed white precipitate was collected by filtration, washed by Et_2O, and stored in a sealed vessel with granulated $CaCl_2$.

The mass concentration of lead in the complex was determined by complexometric titration. The concentration of ceftriaxone in the phosphate buffer solution of [Pb(Ceftria)]·3H_2O was determined by spectrophotometric method using an Analytik Jena Specol 1300 spectrophotometer. The two absorption maxima at 240 nm ($\varepsilon = 30{,}594\ \mathrm{L\,M^{-1}\,cm^{-1}}$) and 270 nm ($\varepsilon = 27{,}825\ \mathrm{L\,M^{-1}\,cm^{-1}}$) in the UV–vis spectra of the ceftriaxone phosphate buffer solution (pH 6.5) were used to plot a calibration curve of optical density *versus* concentration. The absence of sodium and nitrate ions was confirmed with a Thermo Scientific ICAP 6500 spectrometer and Kapel-104T capillary electrophoresis system. Thermogravimetric analysis (TGA) was performed in argon with a simultaneous thermal analyzer NETZSCH STA-409 PC from 20 to 350 °C with a scan rate of 10 °C $\mathrm{min^{-1}}$. FT-IR and Raman spectra of the ceftriaxone disodium salt and [Pb(Ceftria)]·3H_2O were recorded in KBr pellets ranging from 4000 to 400 $\mathrm{cm^{-1}}$ with a Nicolet 6700 spectrophotometer (FT-Raman module coupled with Continuum microscope). The characteristic vibrational frequencies were assigned using methodology described [33]. X-ray analysis of the synthesized compound was performed using an X-ray diffractometer "X'Pert Pro" of "PANalytical" company.

2.2. *Computational methods*

Full conformation analysis was carried out using CONFLEX 6.0 program with MMFF94s molecular mechanics force field and Newton–Raphson method for geometry optimization [34, 35]. The geometry optimization and harmonic vibrational frequency calculations on the most stable conformers were performed with B3LYP [36] and PBE0 [37] density functionals in combination with SBKJC(*p*,*d*) basis set [38, 39] augmented with *s* and *p* diffuse functions, as implemented in the GAMESS suite of electronic structure programs [40, 41]. The relativistic effective core potential (ECP) was used for Pb. The applicability of this basis set and ECP to lead complexes was demonstrated earlier [42]. The Grimme's D3 dispersion

correction was used in all DFT calculations [43]. The partial atomic charges were obtained from Mulliken population analysis. All molecular structures were visualized by the ChemCraft program.

2.3. *Antibacterial activity*

The antibacterial activities of the compounds were tested *in vitro* against Gram-positive bacterium *Staphylococcus aureus* 25923 and Gram-negative bacteria *Escherichia coli* 25922 and *Klebsiella pneumoniae* 13883. The effects of ceftriaxone and [Pb(Ceftria)]·3H_2O on the bacteria were investigated using the paper disk diffusion method [44]. The method included the following steps: (1) preparation of the Mueller–Hinton growth medium; (2) preparation of the micro-organism suspensions of a 0.5 McFarland standard (final concentration 1×108–2×10^8 CFU mL^{-1}); (3) inoculation; (4) pouring the nutrient agar onto a plate and its solidification; (5) dropwise addition of the test substance to a 10 mm diameter filter paper disk placed at the center of each agar plate followed by incubation; and (6) measuring the diameters of the inhibition zones. The bacteria were cultured in an incubator for 18–24 h at 36 °C. Standard disks were impregnated with the solutions of the compounds in phosphate buffer (pH 6).

3. Results and discussion

3.1. *Structure and composition determination*

According to the X-ray powder diffraction analysis, the obtained complex is amorphous. It is insoluble in water as well as in EtOH and acetone. The TGA shows a mass loss of 5.35% from 50 to 145 °C, which is equivalent to three water molecules (figure 2). The endothermic peak at 75 °C on the differential scanning calorimetry (DSC) curve is also caused by water removal. The mass losses at 290 °C correspond to exothermic effect associated with decomposition of ceftriaxone. The composition of the synthesized complex obtained from experiments (complexometric titration, spectrophotometric analysis, and

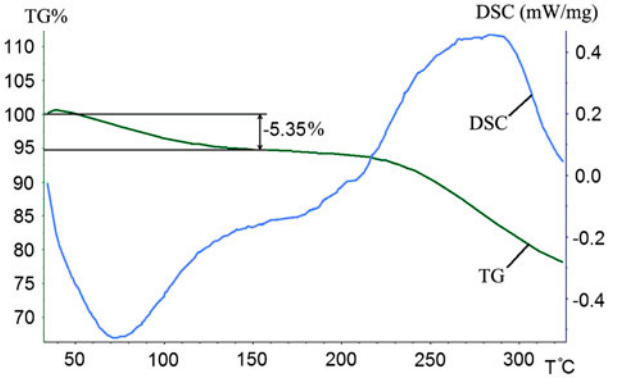

Figure 2. DSC of [Pb(Ceftria)]·3H_2O.

TGA) is in good agreement with stoichiometric calculation based on $[Pb(Ceftria)]\cdot 3H_2O$ chemical formula (table 1). The capillary electrophoresis and chemical analysis of $[Pb(Ceftria)]\cdot 3H_2O$ indicates the absence of nitrate and sodium ions. Thus, the electroneutrality of the complex is caused by sodium ion substitution with lead ions. The complexometric

Table 1. Composition of $[PbL_n]\cdot mH_2O$ (L=Ceftria) complexes reported as mass fraction (ω) of the components.

Component	ω, % (Experiment)	ω, % (Stoichiometry)					
		$[PbL]\cdot 3H_2O$	$[PbL]\cdot 2H_2O$	$[PbL]\cdot H_2O$	$[PbL_2]\cdot 3H_2O$	$[PbL_2]\cdot 2H_2O$	$[PbL_2]\cdot H_2O$
Pb(II)	25.0 ± 1.5	25.5	26.0	26.6	15.2	15.4	15.6
Ceftriaxone	66.3 ± 3.3	67.9	69.4	71.0	80.9	82.0	83.1
H_2O	5.35	6.6	4.5	2.3	4.0	2.7	1.4

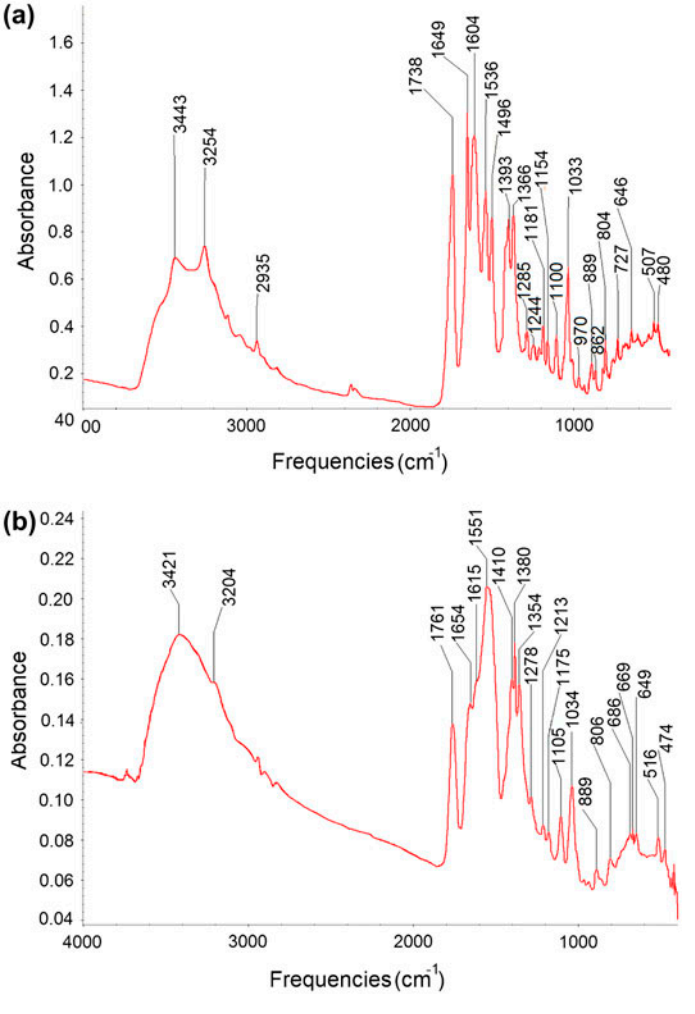

Figure 3. IR spectra of ceftriaxone disodium salt (a); and $[Pb(Ceftria)]\cdot 3H_2O$ (b).

Table 2. Experimental IR frequencies of Na_2Ceftria and [Pb(Ceftria)]·$3H_2O$.

Functional group	Na_2Ceftria, cm^{-1}	[Pb(Ceftria)]·$3H_2O$, cm^{-1}
ν(C=O)-lactam	1738	1761
$\nu_s(COO^-)$	1393	1380
ν(C–O)-triazine	1536	1551

titration showed 25 ± 1% of lead, which should be compared with 25.5% calculated from [Pb(Ceftria)]·$3H_2O$ stoichiometry. Spectrophotometric determination of ceftriaxone indicates that the complex contains 66 ± 3% of ceftriaxone, which is in agreement with 67.9% calculated from [Pb(Ceftria)]·$3H_2O$ stoichiometry. The Pb(II) and Na_2Ceftria precipitate from the aqueous solution of the complex with molar ratio of Pb(II) : Na_2Ceftria = 1 : 1.

To establish the type of ceftriaxone coordination to lead ion, the FT-IR spectra of disodium ceftriaxone and [Pb(Ceftria)]·$3H_2O$ (figure 3) were analyzed. There are three important absorption bands associated with the stretching vibrations of several functional groups participating in the complex formation (table 2). After ceftriaxone coordination to lead ion, the frequencies of the ν(C=O)-lactam and ν(C=O)-triazine modes shift from 1738 to 1761 cm^{-1} and from 1536 to 1551 cm^{-1}, respectively. The increase in the vibrational frequencies of carbonyl groups can be explained by oxygens of lactam and triazine coordinating to Pb(II) and leading to the formation of a chelate complex. These intramolecular interactions between oxygen and lead ion result in more rigid molecular structure around the oxygen and shift of carbonyl vibrational frequencies to higher wavenumbers. The frequency of the symmetric stretching mode $\nu_s(COO^-)$ shifts from 1393 to 1380 cm^{-1}. These shifts indicate that the carboxylate group (COO), the lactam carbonyl group (C=O), and the oxo group of the triazine ring are involved in the formation of [Pb(Ceftria)]·$3H_2O$. This analysis is in agreement with previous studies where ceftriaxone is described as a polydentate ligand [45, 46]. The broad band in the [Pb(Ceftria)]·$3H_2O$ spectrum at 1654 and 1615 cm^{-1} has a high intensity and a low resolution due to the overlap of several vibrational modes, including ν(C=O)-amide, ν(C=O)-triazine, ν_{as}(COO–), ν(C=C), and ν(C=N). Therefore, the small frequency shifts from 1604 to 1615 cm^{-1} and from 1649 to 1654 cm^{-1} cannot serve as sufficient evidence that all these groups participate in complex formation. The Raman spectra also are in agreement with FT-IR spectra of the [Pb(Ceftria)]·$3H_2O$ complex.

3.2. *Computational studies*

To determine the structure of the first coordination sphere of [Pb(Ceftria)], we performed molecular mechanics and quantum chemical calculations. In the first stage, the conformational search for ceftriaxone was carried out with molecular mechanic force field. The results show that at 298 K ceftriaxone has 636 conformational isomers. We focused on nine conformers with relative steric energies between 0 and 2 kcal M^{-1} that accounts for 95.61% of all conformers. Next, based on analysis of the FT-IR spectra and the capillary electrophoresis data, we identified conformers with close spatial positions of the atoms involved in the ligand–metal bond formation. Analysis of the FT-IR spectra indicates that the carboxylate, the lactam carbonyl, and the oxo group of the triazine ring are involved in the formation of [Pb(Ceftria)] complex. Thus, requirement for close spatial positions of lactam carbonyl, triazine, and carboxylate groups led to reduction of the number of conformers. In the end, only two conformers (s-trans–s-cys and s-cys–s-cys) of $Ceftria^{2-}$ and its substituents, with sufficiently large cavity for Pb(II), were considered (figure 4).

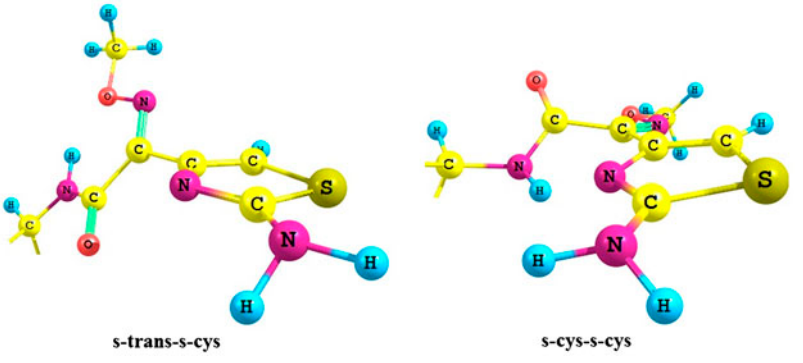

Figure 4. Structures of the ceftriaxone dianion conformers s-trans–s-cys and s-cys–s-cys. Only fragments different in the two conformers are shown.

The geometries of the two Ceftria^{2-} dianions in the most stable conformations were optimized with B3LYP density functional theory. The B3LYP calculations indicate that the s-cys–s-cys conformer is more energetically favorable than the s-trans–s-cys conformer by 5.9 kcal M^{-1}. These conformers differ by rotation of methoxyimino group around the C–C bond. In particular, in the s-trans–s-cys conformer, the planar methoxyiminoacetyl and 2-amino-1,3-thiazol-4-yl are rotated by 58° with respect to each other. In the s-cys–s-cys conformer, the distortion of the methoxyiminoacetyl, with oxygen moved out of methoxyiminoacetyl plane, is observed. This distortion results in extension of the π-conjugated system and delocalization of the π-electrons of methoxyimino and 2-amino-1,3-thiazol-4-yl groups.

The more energetically favorable s-cys–s-cys conformer was used as a ceftriaxone dianion involved in the lead complex formation. Lead ion was introduced into the ligand cavity in order to determine the nature of the first coordination sphere. The placement of lead ion near donors of ceftriaxone has led to the formation of two distinct complexes (figure 5). In **1**, five ligand atoms form a square pyramid around the lead ion, which is coordinated by N and O of the triazine, the nitrogen of the amine group, and the oxygens of the lactam carbonyl and carboxylate groups. In **2**, the coordination of lead is trigonal bipyramidal. In the first coordination sphere, the O atom of the triazine is replaced by N of the thiazole ring.

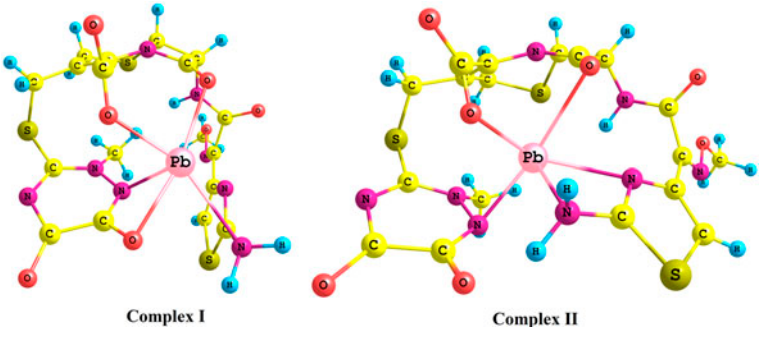

Figure 5. Structures of **1** and **2**.

According to the B3LYP calculations, the square pyramidal coordination of **1** is 10.6 kcal M^{-1} lower in energy than the trigonal bipyramidal coordination of **2**. In **1**, the distance between Pb and O from the lactam carbonyl group is 0.3 Å, shorter than in **2** (figure 6). This results in a significant polarization of the C=O bond and high electron density on the oxygen. The partial charge on the oxygen atom in **1** is −0.419, which is much smaller than −0.332 in **2** (table 3). The charge on the nitrogen of the thiazole ring is smaller in **1** than in ceftriaxone dianion. This change is associated with shifting the electron density of the delocalized π-electrons in the direction of the amino group.

Table 4 summarizes the calculated vibrational frequencies of the two complexes. The average deviations of the B3LYP frequencies from the experimental values are 8.0 and 8.3 cm^{-1} for **1** and **2**, respectively. The maximum absolute deviations are 18 and 39 cm^{-1} for **1** and **2**, respectively. Calculations with PBE0 density functional with the same basis set and dispersion correction give very similar optimized geometries and predict that **1** is 7.7 kcal M^{-1}

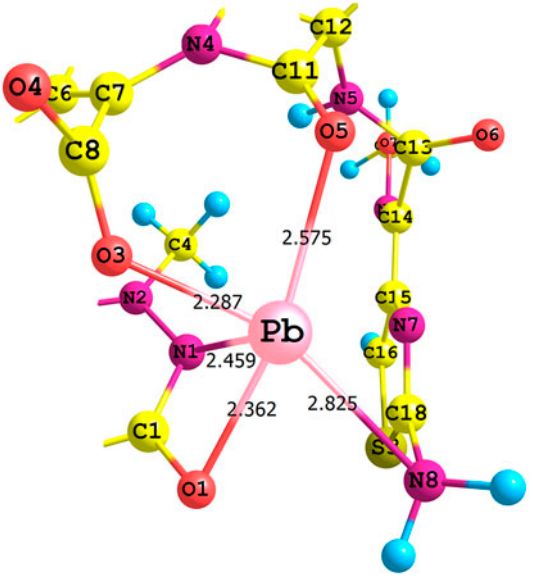

Figure 6. Inner coordination sphere of **1** with bond lengths in Å.

Table 3. Bond orders and atomic charges of **1** and ceftriaxone dianion.

	Atomic charge			Bond order	
Atom	Dianion	Complex **1**	Bond	Dianion	Complex **1**
O5	−0.312	−0.419	O5–C11	1.309	−0.202
O3	−0.496	−0.575	O3–C8	0.956	−0.081
N8	−0.360	−0.445	N8–C18	0.254	0.187
N7	−0.375	−0.324	N7–C18	1.027	0.524
N1	−0.260	−0.314	N7–C15	2.205	1.678
O1	−0.517	−0.512	N1–C1	1.500	1.409
C1	0.181	0.185	N1–N2	−0.138	−0.685
C18	−0.001	−0.106	O1–C1	1.367	1.109

Table 4. Experimental IR and Raman frequencies of Pb(II) with ceftriaxone and calculated B3LYP vibrational frequencies of **1** and **2**, cm^{-1}.

Exp. frequencies		Complex **1**		Complex **2**	
Raman	IR	IR freq.	Functional group	IR freq.	Functional group
1757	1761	1779	ν(C=O) lactam + ν(C=O) amide	1800	ν(C=O) lactam + ν(C=O) amide
1579	1551	1551	ν_{as}(C–N) N–C–N group of triazine + ν(C=O) oxo group at position 6 + $\delta_{as}(CH_3)$ methyl	1554	ν_{as}(C–N) N–C–N group of triazine + ν(C=O) oxo group at position 6 + $\delta_{as}(CH_3)$ methyl
1401	1410	1418	$\delta(CH_2)$ cephem + $\delta_s(CH_3)$ methyl	1405	$\delta_s(CH_3)$ methyl
1401	1380	1375	ν_{as}(C–N) C–N–C group of triazine + δ(CH) lactam, ν_s(COO)	1367	$\delta_s(CH_3)$ methyl + ν_{as}(C–N) C–N–C group of triazine, ν_s(COO)
1355	1354	1365	$\delta_{as}(CH_3)$ methyl + ν_s(C–N) N–C–N group of triazine	1356	δ(CH) lactam at position 6,7 + $\omega(CH_2)$ cephem + $\omega(CH_2)$ thiomethyl + ν(C–N) lactam
1233	1213	1226	δ(CH) lactam at position 6 + $\omega(CH_2)$ thiomethyl	1219	ν_s(C–N) N–C–N group of triazine
1207	1175	1174	$r(CH_3)$ methyl	1177	$r(CH_3)$ methoxy + δ(CH) aminothiazole + δ(NH) amide + ν_{as}(C–N) C–N–C amide
1042	1034	1041	δ(CH) aminothiazole	1036	$\omega(NH_2)$ amine
871	889	898	ν(N–O) methoxy + δ(CH) aminothiazole + δ(CH) lactam at position 6	892	ν(N–O) methoxy + δ(CH) 5-membered ring

lower in energy in comparison with **2**. However, the PBE0 vibrational frequencies are in somewhat worse agreement with the experimental values. The average deviation of the PBE0 frequencies from experimental ones are 13.2 and 15.1 cm^{-1}, with maximum deviations of 34 and 56 cm^{-1} for **1** and **2**, respectively. Nevertheless, both functionals predict that the calculated vibrational frequencies of **1** are in better agreement with the experimental IR frequencies than calculated frequencies of **2**. Therefore, the lower energy of **1** and a better match of its calculated vibrational frequencies with experimental IR frequencies indicate that the structure of the synthesized [Pb(Ceftria)]·$3H_2O$ compound corresponds to **1**.

3.3. *Microbiological screening*

The biological activities of [Pb(Ceftria)]·$3H_2O$ against Gram-positive and Gram-negative bacteria were investigated at the [Pb(Ceftria)]·$3H_2O$ concentrations of 0.4, 0.8, and 1.0 mg mL^{-1}. The effects of [Pb(Ceftria)]·$3H_2O$ on the growth of the bacterial strains *E. coli*, *S. aureus,* and *K. pneumoniae* are summarized in table 5. The biological activity of **1** differs

Table 5. Antibacterial activity of ceftriaxone and [Pb(Ceftria)]·$3H_2O$.

Compound	Concentration, mg mL^{-1}	Zone of inhibition (mm)		
		Klebsiella pneumoniae	*Escherichia coli*	*Staphylococcus aureus*
Na_2Ceftria	0.4	10	29	37
[Pb	1.0	0	41	24
(Ceftria)]·$3H_2O$	0.8	0	39	23
	0.4	0	37	0

from Na_2Ceftria and $Pb(NO_3)_2$ salts. The antibacterial effect of [Pb(Ceftria)]·$3H_2O$ against *E. coli* is present at all concentrations and exceeds the antibacterial effect of Na_2Ceftria by 28% at 0.4 mg mL^{-1}. This enhancement of the antibacterial effect can be simultaneously associated with the action of [Pb(Ceftria)]·$3H_2O$ and its separate components (Pb ion and Ceftria) after decomposition of the complex. According to the spectrophotometric analysis, the phosphate buffer solutions of the complex are stable for about 8 h after the preparation. The zone of inhibition for *E. coli* treated with 0.4 mg mL^{-1} $Pb(NO_3)_2$ salt was 11 mm, indicating a significant resistance of *E. coli* to Pb ion. However, the synergetic effects of ceftriaxone and Pb ion may play an important role in inhibition of bacterial growth after the complex decomposition. These effects are due to the different mechanisms of the action of heavy ions and antibiotics on the bacteria metabolism [47, 48].

At 0.8 and 1 mg mL^{-1}, Na_2Ceftria completely inhibits the bacterial growth, and agar plates contain no *E. coli* after incubation period. Therefore, at concentrations above 0.8 mg mL^{-1}, Na_2Ceftria is more effective than [Pb(Ceftria)]·$3H_2O$. The antibacterial effect against *S. aureus* was present at the [Pb(Ceftria)]·$3H_2O$ concentrations of 0.8 and 1.0 mg mL^{-1} (the inhibition zones are 23 and 24 mm, respectively). These values are 1.5 times smaller than the corresponding values for Na_2Ceftria. Based on these results, *E. coli* and *S. aureus* were classified as sensitive to [Pb(Ceftria)]·$3H_2O$ compound. However, [Pb(Ceftria)]·$3H_2O$ seems to be more potent than Na_2Ceftria against *E. coli*.

Very different results were obtained for *K. pneumoniae*. The zone of inhibition after treatment with Na_2Ceftria salt was 10 mm. According to the standard criteria for evaluation of the drugs, antibacterial action on micro-organisms where such a small zone of inhibition indicates that *K. pneumoniae* is stable with respect to Na_2Ceftria salt. The inhibition zones were completely absent at all used concentrations of [Pb(Ceftria)]·$3H_2O$, indicating resistance of this bacteria to [Pb(Ceftria)]·$3H_2O$ as well.

4. Conclusion

We report the synthesis of [Pb(Ceftria)]·$3H_2O$ by reaction of ceftriaxone disodium salt (hemi)heptahydrate with lead nitrate in water–ethanol medium. TGA indicates that three water molecules form the outer coordination sphere of the complex. The structure of the complex has been studied using FT-IR and UV–vis spectroscopies, capillary electrophoresis, and DFT calculations. The ceftriaxone serves as a pentadentate ligand forming a distorted square pyramidal coordination with lead ion, which is coordinated by N and O of the triazine, nitrogen of the amine, and oxygens of the lactam carbonyl and carboxylate. The antibacterial activity of [Pb(Ceftria)]·$3H_2O$ depends on the bacterial species. The antibacterial activity against *S. aureus* is reduced compared with ceftriaxone. There is no antibacterial activity observed against *K. pneumoniae*. In contrast, compared with ceftriaxone, the antibacterial activity of [Pb(Ceftria)]·$3H_2O$ against *E. coli* increases by 28% at low concentration (0.4 mg mL^{-1}), but decreases at the concentrations above 0.8 mg mL^{-1}.

Acknowledgements

The reported study was supported by RFBR, research project No. 14-03-31,170 мол_а and Krasnoyarsk regional fund for supporting scientific and technological activities. We thank

the Center for Equipment Joint Use of the Siberian Federal University. We are grateful to the HPC Research Departments of Siberian Federal University and Moscow University Supercomputing Center (SKIF MSU «Chebyshev») for the access to the high-performance computer clusters.

Supplemental data

Supplemental data for this article can be accessed here http://dx.doi.org/10.1080/00958972.2014.938065.

References

[1] R. Gaur, M. Azizi, J. Gan, P. Hansal, K. Harper, R. Mannan, A. Panchal, K. Patel, M. Patel, N. Patel, J. Rana, A. Rogowska. *British Pharmacopoeia*, The Stationary Office, London (2009).
[2] R.J. Worthington, C. Melander. *J. Org. Chem.*, **78**, 4207 (2013).
[3] H.M. Owens, A.K. Dash. *Profiles Drug Subst. Excip. Relat. Methodol.*, **30**, 21 (2003).
[4] M. Torres, M. Blanca. *Med. Clin. North Am.*, **94**, 805 (2010).
[5] J.F. Fisher, S.O. Meroueh, S. Mobashery. *Chem. Rev.*, **105**, 395 (2005).
[6] W. Lee, M.A. McDonough, L.P. Kotra, Z.-H. Li, N.R. Silvaggi, Y. Takeda, J.A. Kelly, S. Mobashery. *Proc. Natl. Acad. Sci.*, **98**, 1427 (2001).
[7] J. Fisher, S. Mobashery. *Curr. Prot. Pept. Sci.*, **10**, 401 (2009).
[8] A. Zapun, C. Contreras-Martel, T. Vernet. *FEMS Microbiol. Rev.*, **32**, 361 (2008).
[9] J.S. Bradley, R.T. Wassel, L. Lee, S. Nambiar. *Pediatrics*, **123**, e609 (2009).
[10] M. Babic, A.M. Hujer, R.A. Bonomo. *Drug Resist. Updates*, **9**, 142 (2006).
[11] G.A. Jacoby, A.A. Medeiros. *Antimicrob. Agents Chemother.*, **35**, 1697 (1991).
[12] G.A. Jacoby, L.S. Munoz-Price. *New Engl. J. Med.*, **352**, 380 (2005).
[13] K. Bush. *Clin. Infect. Dis.*, **27**, S48 (1998).
[14] P. Oelschlaeger. *J. Inorg. Biochem.*, **102**, 2043 (2008).
[15] R.M. Breece, L.I. Llarrull, M.F. Tioni, A.J. Vila, D.L. Tierney. *J. Inorg. Biochem.*, **111**, 182 (2012).
[16] S.M. Drawz, R.A. Bonomo. *Clin. Microbiol. Rev.*, **23**, 160 (2010).
[17] H.F. Chambers. *J. Infect. Dis.*, **179**, S353 (1999).
[18] L.D. Bowler, Q.Y. Zhang, J.Y. Riou, B.G. Spratt. *J. Bacteriol.*, **176**, 333 (1994).
[19] K. Bush. *Clin. Microbiol. Rev.*, **1**, 109 (1988).
[20] A.A. Medeiros. *Clin. Infect. Dis.*, **24**, S19 (1997).
[21] I. Sousa, V. Claro, J.L. Pereira, A.L. Amaral, L. Cunha-Silva, B. de Castro, M.J. Feio, E. Pereira, P. Gameiro. *J. Inorg. Biochem.*, **110**, 64 (2012).
[22] M. Arif, M.M.R. Qurashi, M.A. Shad. *J. Coord. Chem.*, **64**, 1914 (2011).
[23] J.R. Anacona, H. Rodriguez. *J. Coord. Chem.*, **62**, 2212 (2009).
[24] J.R. Anacona, A. Rodriguez. *Transition Met. Chem.*, **30**, 897 (2005).
[25] H.-R. Schmutz, P. Detampel, T. Bühler, A. Büttler, B. Gygax, J. Huwyler. *J. Pharm. Sci.*, **100**, 2300 (2011).
[26] D.H. Brown, W.E. Smith, J.W. Teape, A.J. Lewis. *J. Med. Chem.*, **23**, 729 (1980).
[27] J.R. Anacona, C. Patino. *J. Coord. Chem.*, **62**, 613 (2009).
[28] K. Stokowa, W. Szczepanik, N. Gaggelli, E. Gaggelli, G. Valensin, M. Jeżowska-Bojczuk. *J. Inorg. Biochem.*, **106**, 111 (2012).
[29] K. Stokowa-Sołtys, N. Gaggelli, J. Nagaj, W. Szczepanik, J. Ciesiołka, J. Wrzesiński, A. Górska, E. Gaggelli, G. Valensin, M. Jeżowska-Bojczuk. *J. Inorg. Biochem.*, **124**, 26 (2013).
[30] L. Aristilde, G. Sposito. *Environ. Toxicol. Chem.*, **27**, 2304 (2008).
[31] A. Fattah, M. El-Walily, A.A. Gazy, S.F. Belal, E.F. Khamis. *J. Pharm. Biomed. Anal.*, **22**, 385 (2000).
[32] L.I. Bebawy, K. Kelani, L.A. Fattah. *J. Pharm. Biomed. Anal.*, **32**, 1219 (2003).
[33] K. Nakamoto. *Infrared and Raman Spectra of Inorganic and Coordination Compounds*, Wiley, New York (2009).
[34] H. Goto, E. Osawa. *J. Am. Chem. Soc.*, **111**, 8950 (1989).
[35] H. Goto, E. Osawa. *J. Am. Chem. Soc., Perkin Trans.*, **2**, 187 (1993).
[36] A.D. Becke. *J. Chem. Phys.*, **98**, 5648 (1993).
[37] C. Adamo, V. Barone. *J. Chem. Phys.*, **110**, 6158 (1999).
[38] J.S. Binkley, J.A. Pople, W.J. Hehre. *J. Am. Chem. Soc.*, **102**, 939 (1980).
[39] W.J. Stevens, H. Basch, M. Krauss. *J. Chem. Phys.*, **81**, 6026 (1984).

[40] M.W. Schmidt, K.K. Baldridge, J.A. Boatz, S.T. Elbert, M.S. Gordon, J.H. Jensen, S. Koseki, N. Matsunaga, K.A. Nguyen, S. Su, T.L. Windus, M. Dupuis, J.A. Montgomery Jr. *J. Comput. Chem.*, **14**, 1347 (1993).
[41] M.S. Gordon, M.W. Schmidt. In *Theory and Applications of Computational Chemistry: The First Forty Years*, C.E. Dykstra, G. Frenking K.S. Kim, G.E. Scuseria (Eds), pp. 1167–1189, Elsevier, Amsterdam (2005).
[42] A.T. Kowal. *J. Mol. Struct. Theochem.*, **761**, 119 (2006).
[43] S. Grimme, J. Antony, S. Ehrlich, H. Krieg. *J. Chem. Phys.*, **132**, 154104 (2010).
[44] D. Liu, K. Kwasniewska. *Bull. Environ. Contam. Toxicol.*, **27**, 289 (1981).
[45] S. Fu, Z. Liu, S. Liu, A. Yi. *Talanta*, **75**, 528 (2008).
[46] A.E. Ali. *Spectrochim. Acta, Part A*, **78**, 224 (2011).
[47] L. Peng, R. Lifang, X. Hongyu, L. Xi, Z. Chaocan. *Biol. Trace Elem. Res.*, **115**, 195 (2007).
[48] A. Yotsuji, J. Mitsuyama, R. Hori, T. Yasuda, I. Saikawa, M. Inoue, S. Mitsuhashi. *Antimicrob. Agents Chemother.*, **32**, 1097 (1988).